



HAL
open science

Dynamics of Mixed Clathrate-Ice Shells on Ocean Worlds

Evan Carnahan, Steven D. Vance, Marc A. Hesse, Baptiste Journaux,
Christophe Sotin

► **To cite this version:**

Evan Carnahan, Steven D. Vance, Marc A. Hesse, Baptiste Journaux, Christophe Sotin. Dynamics of Mixed Clathrate-Ice Shells on Ocean Worlds. *Geophysical Research Letters*, 2022, 49, 10.1029/2021GL097602 . insu-03663665

HAL Id: insu-03663665

<https://insu.hal.science/insu-03663665>

Submitted on 18 Aug 2022

HAL is a multi-disciplinary open access archive for the deposit and dissemination of scientific research documents, whether they are published or not. The documents may come from teaching and research institutions in France or abroad, or from public or private research centers.

L'archive ouverte pluridisciplinaire **HAL**, est destinée au dépôt et à la diffusion de documents scientifiques de niveau recherche, publiés ou non, émanant des établissements d'enseignement et de recherche français ou étrangers, des laboratoires publics ou privés.

Copyright

Geophysical Research Letters®

RESEARCH LETTER

10.1029/2021GL097602

Key Points:

- Methane clathrates formed within ocean worlds become entrained throughout their ice shells
- Entrained clathrates slow convection and thicken the conductive lid of outer ice shells on Titan and Pluto
- Clathrate entrainment may stop convective motion in many ocean worlds

Supporting Information:

Supporting Information may be found in the online version of this article.

Correspondence to:






E. Carnahan,
evan.carnahan@utexas.edu

Citation:

Carnahan, E., Vance, S. D., Hesse, M. A., Journaux, B., & Sotin, C. (2022). Dynamics of mixed clathrate-ice shells on ocean worlds. *Geophysical Research Letters*, 49, e2021GL097602. <https://doi.org/10.1029/2021GL097602>

Received 21 DEC 2021
Accepted 29 MAR 2022

Dynamics of Mixed Clathrate-Ice Shells on Ocean Worlds

Evan Carnahan^{1,2,3} , Steven D. Vance⁴ , Marc A. Hesse^{1,2,3} , Baptiste Journaux⁵ , and Christophe Sotin⁶ 

¹Oden Institute for Computational Engineering and Sciences, The University of Texas at Austin, Austin, TX, USA, ²Center for Planetary Systems Habitability, The University of Texas at Austin, Austin, TX, USA, ³Department of Geological Sciences, Jackson School of Geosciences, The University of Texas at Austin, Austin, TX, USA, ⁴Jet Propulsion Laboratory, California Institute of Technology, Pasadena, CA, USA, ⁵Department of Earth and Space Sciences, University of Washington, Seattle, WA, USA, ⁶Laboratoire de Planétologie et Géosciences, Nantes Université, Univ Angers, Le Mans Université, CNRS, UMR 6112, Nantes, France

Abstract The habitability of oceans within icy worlds depends on material and heat transport through their outer ice shells. Previous work shows a methane clathrate layer at the upper surface of the ice shell of Titan thickens the convecting region, while on Pluto a clathrate layer at the base of the ice shell hinders convection. In this way, the dynamics of clathrate-ice shells may be essential to the thermal evolution and habitability of ocean worlds. However, studies to date have not addressed the dynamics that determine the location of clathrates within the ice shell. Here, we show that, in contrast to previous studies, clathrates accumulating at the base of the ice shell are entrained throughout the shell. Clathrates are stiffer than ice. As a result, entrainment slows convection and thickens the conductive lid across a range of ocean worlds, potentially preserving sub-ice oceans but limiting avenues for material transport into them.

Plain Language Summary Icy ocean worlds are promising targets for the discovery of extraterrestrial life in our Solar System. Icy ocean worlds have an outer shell, predominantly composed of ice, which insulates internal oceans where life may exist. Preserving internal oceans depends on the rate of heat loss through the ice shell. Furthermore, the habitability of internal oceans likely depends on the transport of chemical materials from the surface of the ice shell to the ocean below. The outer ice shells of ocean worlds are not exclusively composed of ice. Methane gas released from the core can form methane clathrate hydrates, methane trapped within ice crystals that buoyantly rise to the base of the ice shell. We find, in contrast to previous studies, that clathrates become entrained into the ice shell by convective overturning. Methane clathrates have different physical properties than ice. Entrained clathrates thicken the static region near the surface of the ice shell, limiting avenues for material transport through the ice shell. However, their effect depends on the poorly constrained properties of ice-clathrate mixtures. Finally, we find that clathrate entrainment may altogether halt convective motion in ice shells across a range of ocean worlds, potentially preserving sub-ice oceans.

1. Introduction

Icy bodies with large subsurface oceans, or icy ocean worlds, are prime candidates for extant extraterrestrial life in our Solar System (Hendrix et al., 2019). Planned missions to study the habitability of icy ocean worlds—including Europa, Ganymede, Enceladus, and Titan (Howell & Pappalardo, 2020)—will focus on observing the properties of their geologically active outer shells, which regulate the cooling and material transport into internal oceans. The rate at which ocean worlds cool controls the thickening of the ice shell and thus dictates the preservation of internal oceans. Furthermore, the detection of biomarkers by future missions likely depends on the transport of ocean materials through the ice shell to the near-surface (Trumbo et al., 2019). Thus, the outer shell serves as both a barrier and facilitator for ocean world habitability and the detectability of its potential inhabitants.

The outer ice shells of ocean worlds are expected to consist of primarily water ice, with lesser amounts of other materials. Salts (Buffo et al., 2020; Carlson et al., 1999; Trumbo et al., 2019), salt hydrates (Hand et al., 2006), nitrogen ice (W. B. McKinnon et al., 2016), and volatile clathrates (Choukroun & Sotin, 2012; Hand et al., 2006; Tobie et al., 2006) have been either predicted to exist within or observed on the surfaces of ice shells. Most of these non-ice materials are expected to constitute only small fractions of the outer shell; however, methane clathrates are potentially a major constituent (Bouquet et al., 2019; Kalousová & Sotin, 2020; Kamata et al., 2019;

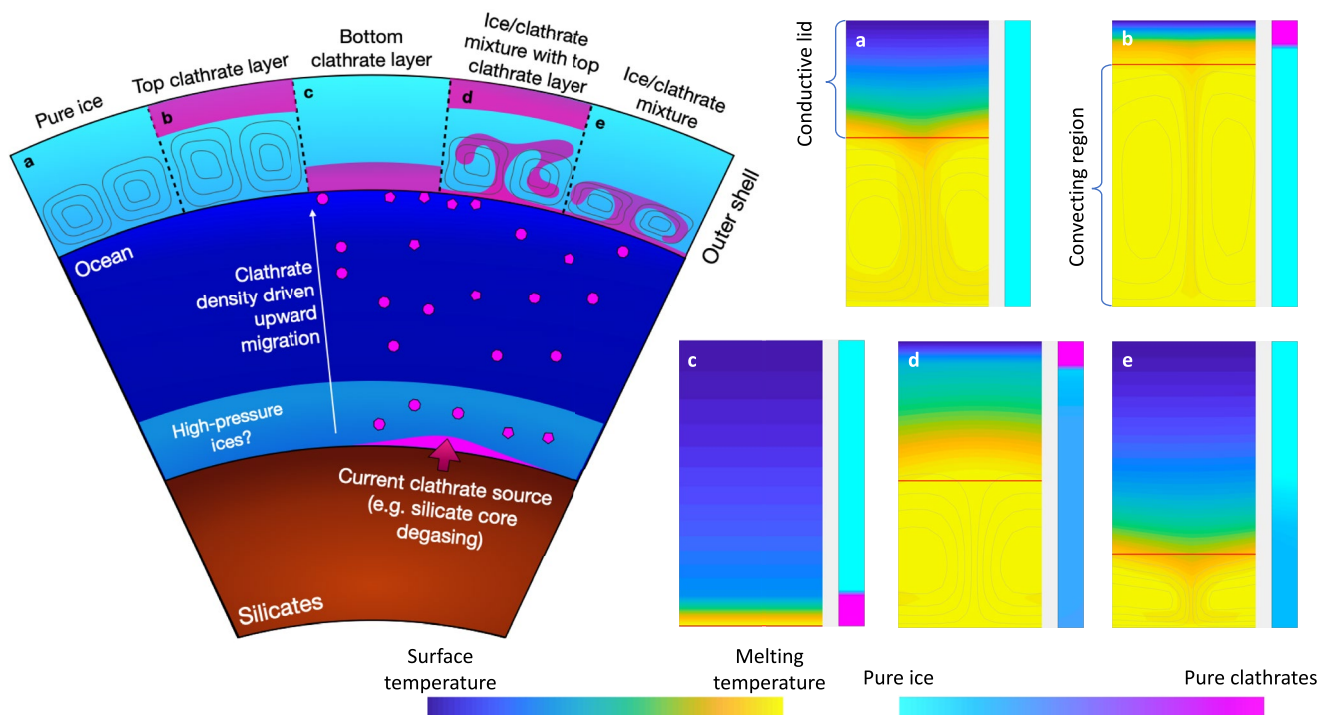


Figure 1. Schematic of modeled icy ocean worlds with mixed clathrate-ice outer shells. Methane clathrates buoyantly rise and are entrained into the outer ice shell. Right: The corresponding thermal structures of mixed outer clathrate-ice shells are shown for (a) a pure ice shell, (b) an ice shell with a surface methane clathrate layer, (c) a pure ice shell with a static basal clathrate layer, (d) a mixed clathrate-ice shell with a surface methane clathrate layer, and (e) a mixed clathrate-ice shell. For each, the average volume fraction of clathrate is plotted and the thickness of the conductive and convective region is marked.

Mousis et al., 2015; Tobie et al., 2006). Recent observations suggest that substantial amounts of clathrate in outer shells are necessary to explain icy bodies' current thermal and elastic structures (Čadek et al., 2021; Choukroun & Sotin, 2012; Fu et al., 2017; Hesse & Castillo-Rogez, 2019; Kamata et al., 2019; Tobie et al., 2006). Methane clathrates preferentially form under the pressure and temperature conditions found in the subsurfaces of icy moons and dwarf planets when dissolved gas concentrations in their oceans are sufficiently high (Choukroun et al., 2013). Furthermore, on Titan methane clathrates can form at the surface from the reaction of water ice with liquid methane, for example, Mousis et al. (2013). Clathrates are expected to be present and stable throughout most of the sub-ice ocean and outer ice shell of a wide range of ocean worlds, including Titan, Pluto, and Europa (Loveday et al., 2001; Mousis et al., 2015). Many mechanisms may result in the formation of methane and methane clathrates throughout planetary evolution (Lunine & Stevenson, 1987; Mousis et al., 2015; Tobie et al., 2006), of these, the breakdown of organic matter is potentially ongoing at present (Miller et al., 2019; Néri et al., 2020). Over long timescales, buoyant methane gas or clathrate will rise to the base of the outer ice shell (Bouquet et al., 2019; Tobie et al., 2006).

The presence of methane clathrates in outer ice shells affects ice shell dynamics and heat transport due to their unique material properties, primarily their higher viscosity (Durham et al., 2003) and lower thermal conductivity (Sloan & Koh, 2007) than ice. However, previous studies have yielded contrary results based on the assumed location of clathrates within the ice shell. On Titan, Kalousová and Sotin (2020) showed that a static methane clathrate layer at the top of the ice shell substantially thins the conductive lid and increases the thickness of the convecting region (Figures 1a and 1b). On Pluto, Kamata et al. (2019) assumed that a mechanically detached, static, methane clathrate layer forms at the base of the outer ice shell and showed that it shuts down convection (Figures 1a and 1c). On Ceres, Formisano et al. (2020) assumed that clathrates are uniformly distributed throughout the ice shell and stabilize the ice shell against convection. These studies demonstrate that the effect of clathrates on ice shell dynamics depends on the assumed location of clathrates within the ice. This finding underscores the importance of understanding how clathrates distribute within the ice. Here, we use numerical simulations to explore how clathrates that form through the continuous release of methane from the interior of

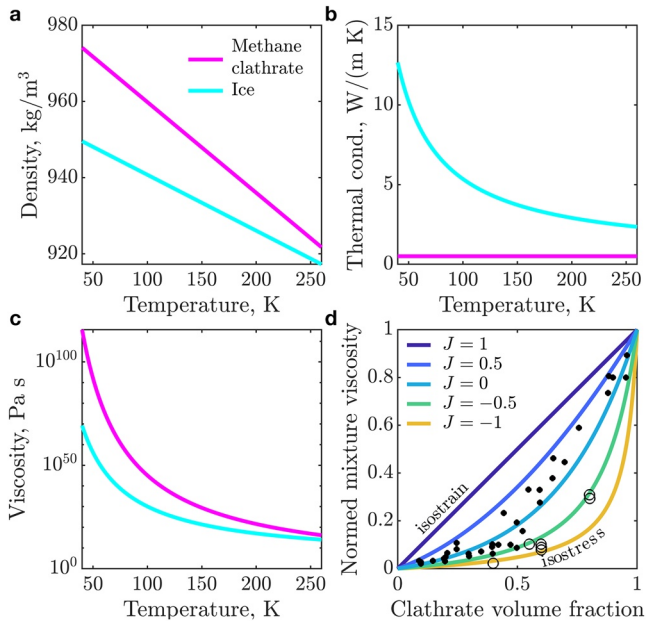


Figure 2. Physical properties of ice and methane clathrate: (a) density at 5 MPa (Feistel & Wagner, 2006; Helgerud et al., 2009), (b) thermal conductivity (Carnahan et al., 2021; Sloan & Koh, 2007), and (c) viscosity (Durham et al., 2003; Goldsby & Kohlstedt, 2001). (d) Viscosity mixing relationships and data for mineral mixtures (Ji, 2004), black dots, and ice-salt hydrate mixtures (Durham et al., 2005), black circles. Viscosities are clathrate-dominant for $J > 0$ and ice-dominant for $J < 0$.

Titan and Pluto distribute within their outer shells, and how this distribution affects ice shell dynamics and heat transport.

2. Methods

2.1. Material Properties

Methane clathrates affect the convective dynamics of an ice shell because they have higher viscosity (Durham et al., 2003; Goldsby & Kohlstedt, 2001), lower thermal conductivity (Carnahan et al., 2021; Sloan & Koh, 2007; Wolfenbarger et al., 2021), and higher density (Feistel & Wagner, 2006; Helgerud et al., 2009) than water ice (Figures 2a–2c). The physical properties of mixtures of ice and methane clathrates depend on the volume fraction of each component. The properties of variable mixtures of clathrates and ice are key to the dynamics of mixed clathrate-ice shells and have not been addressed in previous work on static pure clathrate layers and uniform distributions of clathrates (Formisano et al., 2020; Kalousová & Sotin, 2020; Kamata et al., 2019). A lower bound on the viscosity of a mixture of clathrate and ice is obtained if the same stress is applied to each material (isostress; Figure 2d). An upper bound is obtained if both materials deform at the same rate (isostrain). A general relationship can be established for the properties of mixtures of ice and clathrates,

$$\eta_{\phi} = (\phi\eta_{mc}^J + (1 - \phi)\eta_{ice}^J)^{\frac{1}{J}}; \quad 1 \geq J \geq -1 \quad (1)$$

where ϕ is the volume fraction of methane clathrates (Figure 2d) (Ji, 2004). Here, $J = 1$ recovers the isostrain bound and $J = -1$ the isostress bound (Durham et al., 2003; Neumann et al., 2020).

The theoretical bounds for viscosity mixtures result in vastly different ice shell dynamics, with changes in conductive lid thickness of more than 80 km for Titan (Figure S1 in Supporting Information S1). This high uncertainty should motivate laboratory experiments to constrain the viscosities of clathrate-ice mixtures. Further constraints can be made by drawing analogies to mineral mixtures (Ji, 2004) and ice-salt hydrate mixtures (Durham et al., 2005). Here, most experimental results lie between the less viscous, or in this case, ice dominant rheology, $J = -0.5$, and the more viscous methane clathrate dominant rheology, $J = 0.5$ (Ji, 2004). Mixtures of salt hydrates and ice fit well with $J = -0.5$ (Durham et al., 2005). Theoretical studies of hard inclusions in a soft matrix give results closer to the isostress bound with increasing viscosity contrast (Takeda, 1998). Salt hydrates and ice have viscosity contrasts on the order of 10^5 (Durham et al., 2005) compared to methane clathrates and ice, which in the convecting region have viscosity contrasts on the order of 10^2 (Durham et al., 2003). Due to the high uncertainty in values of J , for example, Moore (2014), we explore the full range of mixture relationships, but we anticipate the value of J for mixtures of methane clathrate and ice mixture to fall between -0.5 and 0.5 .

2.2. Methane Outgassing

We estimate the amount of methane released from the core of Titan in the scenario in which all of the methane gas from the pyrolysis of insoluble organic matter contained in the core is released (Miller et al., 2019). This release of methane gas results in a ~ 40 km layer of methane clathrate around the outside of Titan (Supporting Information S1). For simplicity, we do not evaluate the most plausible methane formation scenario, which likely changed throughout planetary evolution (Lunine & Stevenson, 1987; Miller et al., 2019; Mousis et al., 2015; Néri et al., 2020; Tobie et al., 2006). Instead, we adopt a first-order assumption that methane gas or clathrate emanates from the core at a constant rate throughout planetary evolution, ~ 4 billion years. This assumption provides a reasonable middle ground scenario for the release rate of clathrates and provides a baseline to compare with

scenarios in which clathrates are released on variable timescales. Due to the similarly organic-rich cores of Titan and Pluto (Bardyn et al., 2017; Fulle et al., 2016; W. McKinnon et al., 2017; Néri et al., 2020), and the dearth of specific estimates for the amount of methane on Pluto, we use estimates for the volumes of the cores of Titan and Pluto to volumetrically scale the amount of methane on Titan to Pluto (Robuchon & Nimmo, 2011). We find that a ~ 13 km methane clathrate layer could form on Pluto.

We assume the flux of methane gas or clathrate released from the core over long timescales buoyantly rises through the ocean to the base of the outer ice shell (Bouquet et al., 2019; Tobie et al., 2006). This assumption is predicated on the high relative buoyancy of methane gas and clathrates within ocean worlds (Bouquet et al., 2019; Tobie et al., 2006). However, it is possible that under specific conditions, the rise of clathrates may be halted (Sloan & Koh, 2007).

2.3. Methane Clathrate Incorporation

We do not consider the detailed dynamics for the incorporation of the buoyantly rising methane into the ice shell at the ice-ocean interface. We are not aware of any studies or Earth analogs for this process. There has, however, been significant interest in salt incorporation at the ice-ocean interface, for example, Soderlund et al. (2020). Complex dynamical processes in the mushy layer at the interface leads to the effective desalination of the ice and significantly reduces the salt content (Buffo et al., 2020, 2021; Wells et al., 2019). Methane incorporation, however, is likely different from salt incorporation. First, methane substitutes directly into ice, thereby converting it to clathrate. Second, dissolved methane reduces the brine density rather than increasing it. As such, methane enriched brine would not drain from the mushy layer. Hence, at the macro spatial and temporal scales of our modeling, we assume that all methane incorporates into the ice shell such that clathrates replace ice at the ice-ocean interface. Determining the exact dynamical processes of incorporation requires further study. This first-order approximation of clathrate incorporation is a step beyond assuming that clathrates form separate layers around (Kalousová & Sotin, 2020; Kamata et al., 2019), or appear uniformly throughout (Formisano et al., 2020), an ice shell.

As stated above, we assume that methane, or methane clathrate, incorporates into the ice shell at the base so that clathrates replace existing ice. The change in ice shell volume is therefore the density ratio of $\rho_{\text{ice}}/\rho_{\text{mc}} \sim 0.995$. We neglect this small change in volume as well as the potential for incorporated clathrates to thicken or thin the ice shell in order to keep simulations on a fixed domain. We do, however, explore the effects of variability in ice shell thickness in Section 2.5. By the end of the simulation, all of the released methane is contained within the ice shell as methane clathrate. The entire region where clathrates reside in the ice shell is at pressures and temperatures that prevent clathrate dissociation, even if the ice shell contains substantial impurities, for example, $\sim 5\%$ ammonia (Choukroun et al., 2010).

2.4. Governing Equations and Simulations

The governing equations for mixed clathrate-ice shell convection arise from the balance of momentum and energy. We assume an incompressible infinite Prandtl number fluid with the Oberbeck-Boussinesq approximation (Ismail-Zadeh & Tackley, 2010). This leads to the following Stokes and advection-diffusion equations,

$$\nabla \cdot [\eta (\nabla \mathbf{u} + \nabla \mathbf{u}^T)] - \nabla p = \rho g \hat{\mathbf{z}}, \quad (2a)$$

$$\nabla \cdot \mathbf{u} = 0, \quad (2b)$$

$$\rho c_p \frac{\partial T}{\partial t} + \nabla \cdot [\mathbf{u} \rho c_p T - k \nabla T] = G. \quad (2c)$$

Here, the unknowns are the velocity vector \mathbf{u} , pressure p , and temperature T . The gravitational acceleration, g , is assumed to be constant across the ice shell, $\hat{\mathbf{z}}$ is the vertical unit vector, and t is time. The variable properties are the viscosity, η , density, ρ , and thermal conductivity, k . The tidal heating term, G , depends on viscosity and is maximized near the melting temperature viscosity on Titan (Kalousová & Sotin, 2020).

To model the evolution of methane clathrate within the ice shell, we add a conservation equation for methane (Aziz & Settari, 1979). In general, the total mass of methane in the system is given by the sum over its abundance in all phases, p , in the system,

$$C = \sum_p \rho_p \phi_p X_p$$

where ρ_p and ϕ_p are the density and volume fraction of phase p , and X_p is the mass fraction of methane in phase p . Here, we assume that methane partitions only into the clathrate phase so that $C = \rho_{mc} \phi_{mc} X_{mc}$. The diffusivity of methane in clathrates is very low (Peters et al., 2008); therefore we only consider the advective transport of methane by the flow of the methane clathrate due to solid state convection. There is no internal source term for methane clathrate because it is added as a flux through the bottom boundary. Assuming that both ρ_{mc} and X_{mc} are constant and setting $\phi_{mc} \equiv \phi$, we have the following tracer advection equation for the volume fraction of methane clathrates:

$$\frac{\partial \phi}{\partial t} + \nabla \cdot [\mathbf{u}\phi] = 0. \quad (3)$$

The governing Equations 2 and 3 are solved for \mathbf{u} , p , T , and ϕ on a staggered Cartesian mesh in a rectangular grid, with conservative finite differences for the Stokes equation and a finite volume method with flux-limiters for the transport equations. We impose a flux boundary condition for methane at the base of the shell.

We model the evolution of Titan and Pluto's outer ice shells over a 4 billion year period, during which we add, or more specifically incorporate, the total clathrate layer at the bottom boundary of the ice shell at a constant rate. The density of Titan's hydrocarbon rich atmosphere renders clathrates stable at its surface, and a multikilometer clathrate layer may predate the formation of the ice shell (Kalousová & Sotin, 2020; Tobie et al., 2006). We model a total 100-km thick shell on Titan, with a starting composition of a 10-km clathrate layer at the surface and pure ice below (Kalousová & Sotin, 2020). For Pluto, we perform transient simulations for both a 100-km thick pure ice shell and 200-km thick ice shell with a 10-km surface insulating layer composed of, for example, high porosity or nitrogen ice (thermal conductivity, $k \sim 1 \text{ W m}^{-1} \text{ K}^{-1}$; Hammond et al., 2016; Kamata et al., 2019; W. B. McKinnon et al., 2016). We choose these ice shell thicknesses for our simulations as they are near the middle of the estimated thicknesses (Vance et al., 2018), and, along with our chosen values for surface insulating layers, are in line with previous studies of clathrate-ice shells (Kalousová & Sotin, 2020; Kamata et al., 2019). If the ice shell becomes conductive during its evolution, the remainder of the clathrates are added to the base of the ice shell, thickening the shell (Supporting Information S1).

2.5. Mixed-Component Scaling for Planetary Ice Shells

The values of ice shell parameters used in our, and previous, numerical simulations are fundamentally uncertain. We explore this uncertainty using scaling analysis validated by our numerical simulations. The nondimensionalization of Equations 2a–2c and 3 without tidal heating results in four governing dimensionless scales (Supporting Information S1),

$$\phi_c = \frac{F_{mc}}{H_{conv}}, \quad J, \quad \text{Ra}_\phi = \frac{\rho_c g \alpha_c \Delta T H_{ice}^3}{\eta_c \kappa_c}, \quad \text{and} \quad \Theta_i = \frac{T_i}{T_m}. \quad (4)$$

The first dimensionless scale is the characteristic volume fraction of methane clathrates, ϕ_c , where F_{mc} is the thickness of the methane clathrate layer released from the core and H_{conv} is the thickness of the convecting region. Second, is the viscosity mixing exponent, J . Third, is the basal Rayleigh number for the characteristic volume fraction, where the subscript c denotes the characteristic scale for a given property, H_{ice} is the thickness of the underlying ice layer, and α is the thermal expansivity. Characteristic scales in Ra_ϕ are chosen at the basal temperature with the characteristic volume fraction of clathrates and the viscosity mixing exponent, i.e., $\eta_c = \eta(T_m, \phi_c, J)$. Fourth, is the homologous temperature at the interface of the surface insulating layer and the underlying ice, Θ_i , where T_i is the interface temperature. The homologous temperature at the ice-insulating layer interface governs the contrast in material properties across the ice layer. We calculate a regime diagram based on these four parameters that separates the convective versus conductive boundary of ice shells for a wide range of ice shell configurations. We then approximate the four dimensionless parameters for a given clathrate-ice shell and compare the

convective stability found from the scaling analysis—that is, whether the Rayleigh number calculated is above or below the critical Rayleigh number—to the regime of our transient simulations. We find that the scaling analysis accurately predicts the end dynamic state of ~93% of our numerical simulations, which span a range of shell thicknesses, insulating layers, and clathrate fluxes (Supporting Information S1).

The above scaling of planetary ice shell convection allows us to sample the uncertainty in the amount of methane clathrate released and incorporated into the ice shell, the thickness of the shell, the potential presence of a surface insulating layer, and the ice shell surface temperature, all of which vary between ocean worlds, and even in time during planetary evolution. Furthermore, all are fundamentally uncertain quantities at present. We explore the uncertainty in each of these values by uniformly sampling the likely parameter ranges for Titan, Ganymede, Europa, and Pluto (Table S1 in Supporting Information S1). We then calculate the four dimensionless governing parameters (Equation 4) for each of the sampled ice shells and report whether the mixed clathrate-ice shell is convective or conductive at present.

3. Results and Discussion

A flux of clathrates released from the core buoyantly rises to the base of a convecting outer ice shell, where it is continuously entrained into the ice shell (Figures 1d and 1e). This finding contradicts previous work that assumed clathrates would form a mechanically detached static layer beneath a dynamic ice shell (Kamata et al., 2019). The continuous incorporation of clathrates at the base of the ice shell entrains them throughout the convective portion of the shell. The entrainment of methane clathrates throughout planetary evolution until the present can thicken the conductive lid of Titan by over 60 km (Figures 1b and 1d) and may result in limited convection on Pluto (Figure 1e). However, the effect of entrained clathrates depends on both the viscosity of ice and the viscosity of ice-clathrate mixtures. We explore both of these dependencies for Titan and Pluto.

3.1. Titan and Pluto

Geophysical interpretations of gravity fields are nonunique. For Titan's ice shell structure, variations in the gravity of the outer shell can be explained by Airy isostasy, due to varying basal topography of the shell (Hemingway et al., 2013), or Pratt isostasy, due to lateral density differences (Čadek et al., 2021; Choukroun & Sotin, 2012). Basal topography is maintained if the ice shell is fully conductive and the base of the shell is cold (Hemingway et al., 2013), or if convection is limited and the surface expression of convection cells occurs on the spatial scale of gravity anomalies (Richards & Hager, 1984). However, the presence of sufficient impurities to lower basal ice temperatures enough to sustain basal topography is uncertain (Kalousová & Sotin, 2020; Leitner & Lunine, 2019; Mitri et al., 2014; Vance et al., 2018). Alternatively, density differences may appear in convecting ice shells due to lateral variations in shell materials (Čadek et al., 2021), for example, due to the distribution of clathrates.

Figure 3 depicts the predicted behaviors for the outer shells of Titan (upper panels) and Pluto (lower panels). A range of potential viscosity mixing relationships (J) and ice grain sizes (viscosity) are investigated to predict the duration of convection, the present thickness of the conductive lid, and the basal heat flux. On Titan, the entrainment of clathrates into the ice shell thickens the conductive lid for all parameter combinations and may shut down convection (Figures 3a and 3b). Elastic thicknesses concordant with the interpretation of Titan's shape from basal topography (Hemingway et al., 2013) are obtained for large-grain ice and/or clathrate-dominant mixture rheologies ($J > 0$) for both conductive and convective outer shells (Figure 3b). For small-grained ice and/or ice-dominant mixture rheologies ($J < 0$), the thermal structure of the outer shell is consistent with density compensation (Čadek et al., 2021). Due to the low thermal conductivity of clathrates, only convective solutions provide the required heat flow (Figure 3c). As such, both the thermal (Kalousová & Sotin, 2020) and elastic (Čadek et al., 2021; Hemingway et al., 2013) constraints on Titan may be satisfied by convecting clathrate-ice shells with thick conductive lids.

Pluto's Sputnik Planitia basin has a positive gravity anomaly (Nimmo et al., 2016). To preserve such an anomaly, a sub-ice ocean has been invoked below a locally thinned ice shell. However, unlike some icy moons in the outer Solar System, Pluto has been predicted to have negligible tidal heating; the only significant heat source to sustain an ocean is radiogenic (Bagheri et al., 2022). Prior work (Kamata et al., 2019) finds that a mechanically detached layer of methane clathrates beneath a convecting ice shell will shut down convection and can preserve a sub-ice ocean, but only if enough methane clathrate is available to balance the heat flux. For a thin, 100-km, ice shell, we

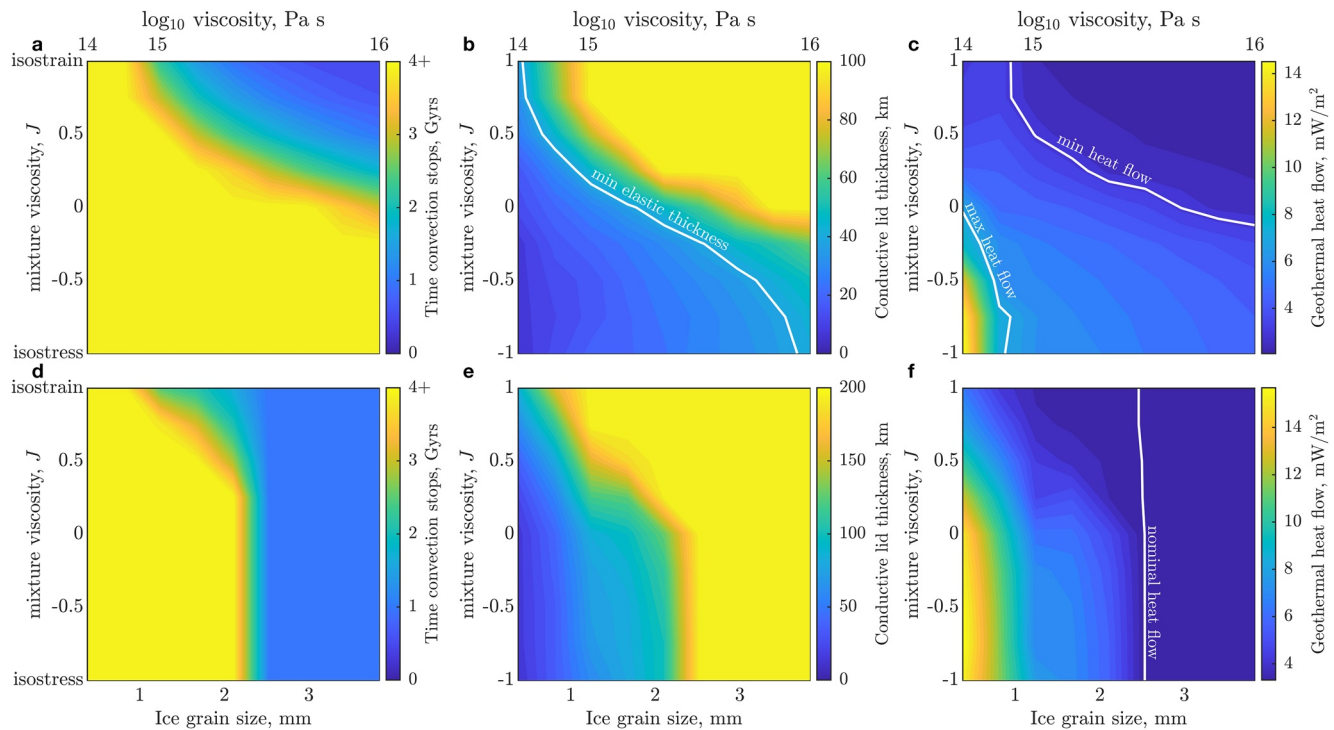


Figure 3. Influence of methane clathrates on the outer shell dynamics of Titan and Pluto for the plausible range of basal ice grain sizes and viscosity mixing relationships. For Titan, contours are plotted for (a) the time until convection stops, (b) conductive lid thickness at present, and (c) geothermal heat flux at present are shown. Similarly for Pluto (d–f). White contour lines depict constraints on the current mechanical structure from the interpretation of Titan's gravity from basal topography (Hemingway et al., 2013) (b) and heat flow (Kalousova & Sotin, 2020) (c). For Pluto, the white contour line in (f) depicts constraints on the present heat flow, $\sim 3.25 \text{ mW/m}^2$ (W. McKinnon et al., 1997; W. B. McKinnon et al., 2016). Simulations of Titan assume a 100-km shell with a 10-km surface clathrate layer. Simulations for Pluto have a 200-km shell with a 10-km surface insulating layer (Methods).

predict that the required inventory of methane is double the estimated amount of methane in the core of Pluto. In addition, we find that a thin convecting ice shell entrains clathrates throughout, and will not stop convecting unless mixture-rheologies are clathrate-dominant (Figure S2 in Supporting Information S1).

For a thick 200-km ice shell on Pluto, clathrates shut down convection if ice grains are on the order of mm in size and clathrates dominate mixture rheologies ($J > 0$; Figures 3d and 3e). Initially convective ice shells entrain clathrates, limiting their overall insulating effect, resulting in heat fluxes above those expected on Pluto (Figure 3f). For ice grains larger than 2.5 mm, the ice shell is initially conductive (Figure 3e) and clathrates will form a separate static layer below the ice shell. In this scenario, the basal heat flow is low enough to sustain a sub-ice ocean with the estimated amount of methane on Pluto (Figure 3f). Finally, we find that a thin basal clathrate layer lowers the ice shell temperature, increasing its viscosity sufficiently to allow the ice to sustain lateral thickness contrasts and preserve a positive gravity anomaly below Sputnik Planitia for nearly a billion years (Kamata et al., 2019; Nimmo et al., 2016).

3.2. Mixed-Component Outer Shells Across Ocean Worlds

A flux of entrained clathrates increases the number of dimensionless numbers controlling the convective stability of an ice shell from two to four (Equation 4). However, the convective regime is still largely controlled by Ra_ϕ and Θ_i . The parameters exclusive to mixed component ice shells, ϕ_c and J , alone have a minimal effect on convective stability; the combined effect of changing J from -0.5 to 0.5 and ϕ_c from 0 to 0.9 is less than half an order of magnitude change in the critical Rayleigh number for convection (Figure S4 in Supporting Information S1). Yet the value of J and ϕ_c also affects the calculation of Ra_ϕ , primarily by changing the value of the characteristic basal viscosity by up to an order of magnitude. A surface insulating layer changes the value of Θ_i , which can reduce the critical Rayleigh number for the onset of convection by over three orders of magnitude (Figure S4 in Supporting Information S1). As a result, we find that the convective stability of an ice shell with an insulating layer and a

Table 1

Percent of Sampled Outer Shells That Are Convective at Present Day for Titan, Pluto, Europa, and Ganymede for a Pure Ice Shell; an Ice Shell With Only a Surface Insulating Layer; and an Ice Shell With a Surface Insulating Layer and Entrained Clathrates for Two Different Mixture Rheologies, Ice-Dominant ($J = -0.5$) and Clathrate-Dominant ($J = 0.5$) Viscosity Mixtures

	H (km)	H_{mc} (km)	H_{rel} (km)	Pure ice shell	Insulating surface layer	Surface layer and clathrates	
						($J = -0.5$)	($J = 0.5$)
Titan	50–170	5–20	20–39	66	95	87	43
Pluto	100–330	0–5	6–12	51	60	60	49
Europa	5–90	0–10	17–34	14	47	30	17
Ganymede	25–160	0–10	16–23	40	64	57	22

Note. Sampled outer shells are from likely shell parameters (Supporting Information S1). Shown are the sampled range of ice shell thicknesses, H (Kamata et al., 2019; Robuchon & Nimmo, 2011; Vance et al., 2018; Vilella et al., 2020); methane clathrate surface layers on Titan (or general surface insulating layers for Pluto, Europa, and Ganymede), H_{mc} (Hammond et al., 2016; Kalousova & Sotin, 2020; Kamata et al., 2019); and total thickness of a methane clathrate layer released from the core, H_{rel} (Miller et al., 2019).

basal flux of clathrates is largely determined by changes in Ra_ϕ and Θ_i . Here, Θ_i is predominantly determined by the thickness of the surface insulating layer, whereas Ra_ϕ is primarily influenced by the thickness of the ice layer and the viscosity of the clathrate ice-mixture at the base of the shell.

Employing our scaling of clathrate-ice shells, we sample the uncertainty in relevant ice shell parameters for Titan, Pluto, Europa, and Ganymede (Table S1 in Supporting Information S1) and predict what fraction of ice shells will be convective before and after clathrates are entrained in the outer shell (Table 1) by comparing the calculated Rayleigh number for each sample to the critical Rayleigh number. Pure ice layers on Europa are likely conductive due to the lower expected shell thickness, whereas the thicker predicted shells on Titan are convecting (Carnahan et al., 2021; Howell, 2021). The presence of a surface clathrate layer insulates the underlying ice, resulting in a greater proportion of convective profiles for any given world (Table 1). The addition of a basal flux of clathrates entrained within the ice shell reduces the chances of convection on all ocean worlds. However, with less viscous ice-dominant mixture rheologies ($J = -0.5$) ice shells are only marginally more likely to be conductive with entrained clathrates. For clathrate-dominant mixture rheologies ($J = 0.5$) a majority of parameter combinations for ice shells on all ocean worlds explored are conductive.

Our numerical simulations show that both Pratt and Airy interpretations of Titan's gravity are possible (Čadek et al., 2021; Hemingway et al., 2013) (Figure 3). However, the large spatial scale of gravity variations suggests that convection cells alone cannot produce the observed pattern (Hemingway et al., 2013). Thus, the outer shell must be fully conductive for the gravity to be explained by variations in basal topography. For ice-dominant mixture rheologies ($J = -0.5$), the majority of parameter combinations for the outer shell of Titan are convecting; for even the upper bound clathrate-dominant rheologies ($J = 0.5$) roughly half the parameter combinations sampled are convecting (Table 1). This finding suggests that gravity variation on Titan occurs from lateral density changes in the outer shell, that is, Pratt isostasy (Čadek et al., 2021; Choukroun & Sotin, 2012).

Other materials with similar properties to methane clathrate (e.g., thermal conductivity, density, and rheology) may be present in the ice shells of ocean worlds (Hand et al., 2006) and exoplanets (Marounina & Rogers, 2019). Surface insulating layers in outer shells may come in the form of nitrogen ice (Nimmo et al., 2016), porosity (Hammond et al., 2016; Nimmo et al., 2003), or hydrated salts (Hand et al., 2006). All of these impurities have lower thermal conductivity than ice and will increase the likelihood of convection in the underlying ice shell. Other volatile clathrates are expected to be present and to rise buoyantly to the base of the outer shell (Bouquet et al., 2019), where they will be entrained into the convecting ice. The entrainment into the ice of buoyant volatile clathrates will reduce convection in ice shells due to their high viscosity (Durham et al., 2010; Formisano et al., 2020). Accounting for mixed-component outer shells can improve the interpretation of surface observations of icy bodies that suggest more viscous outer shells (Fu et al., 2017; Hemingway et al., 2013) and slow cooling (Hesse & Castillo-Rogez, 2019; Nimmo et al., 2016). Finally, analogous to the effects in outer shells, mixed

components will also affect the dynamics of internal high-pressure ice layers, which regulate the thermal and geochemical transport from the core to the ocean on large ocean worlds (Journaux, Kalousová, et al., 2020).

4. Conclusions

We evaluate the dynamics that dictate the location of clathrates within the outer ice shell of ocean worlds. We find that methane clathrates formed from a continuous methane supply and incorporated into the base of the ice shell become entrained throughout the convective portion of outer shells. This entrainment thickens the conductive lid and limits heat flow out of ocean worlds. However, the influence of clathrates on ice shell dynamics is largely controlled by the poorly constrained viscosity of clathrate-ice mixtures. On Titan, we find the current thermal and elastic constraints may be satisfied by sluggishly convecting clathrate-ice shells. On Pluto, entrained clathrates do not shut down convection unless clathrates dominate the mixture viscosity. Furthermore, clathrate entrainment limits their overall effect on heat flow. A thin subsurface ocean on Pluto can only be maintained if convection is suppressed by highly viscous large grained ice. This lack of motion prevents the entrainment of clathrates and allows the formation of a pure clathrate layer at the base of the ice shell. We develop a scaling for mixed component ice shells, which shows that when insulating layers are present at the surface of an ice shell, they dramatically increase the likelihood of convection, whereas entrained clathrates substantially limit convection on ocean worlds. Across a wide a range of ocean worlds the transient entrainment of clathrates until the present may altogether shut down convection. The pronounced effect of clathrates on heat transport has the potential to preserve sub-ice ocean habitats, while simultaneously limiting avenues for habitability promoting material transport through the ice shell.

Data Availability Statement

The numerical model used in this study can be found at <https://doi.org/10.5281/zenodo.6403015> along with a few demo simulations and the code and data to create the modeling results figure.

Acknowledgments

Part of the research was carried out at the Jet Propulsion Laboratory, California Institute of Technology, under a contract with the National Aeronautics and Space Administration (80NM0018D0004). Work by E. Carnahan, S. D. Vance, and C. Sotin was supported by the NASA Astrobiology Institute's Hydrocarbon Worlds project (17-NAI8-0017). M. A. Hesse was supported by National Science Foundation (NSF) Grant DMS-172034 and acknowledges support for publication costs from the Department of Geological Science Owen Coats fund. The authors thank Angela Marusiak, Mohit Daswani, Natalie Wolfenbarger, and Kristopher Darnell for discussions that improved this manuscript. This is UT Center for Planetary Systems Habitability Contribution #0052.

References

- Aziz, K., & Settari, A. (1979). *Petroleum reservoir simulation*. Applied Science Publishers.
- Bagheri, A., Khan, A., Deschamps, F., Samuel, H., Kruglyakov, M., & Giardini, D. (2022). The tidal–thermal evolution of the Pluto–Charon system. *Icarus*, 376, 114871. <https://doi.org/10.1016/j.icarus.2021.114871>
- Bardyn, A., Baklouti, D., Cottin, H., Fray, N., Briois, C., Paquette, J., et al. (2017). Carbon-rich dust in comet 67P/Churyumov-Gerasimenko measured by COSIMA/Rosetta. *Monthly Notices of the Royal Astronomical Society*, 469, S712–S722. <https://doi.org/10.1093/mnras/stx2640>
- Bouquet, A., Mousis, O., Glein, C. R., Danger, G., & Waite, J. H. (2019). The role of clathrate formation in Europa's ocean composition. *The Astrophysical Journal*, 885(1), 14. <https://doi.org/10.3847/1538-4357/ab40b0>
- Buffo, J. J., Meyer, C. R., & Parkinson, J. R. (2021). Dynamics of a solidifying icy satellite shell. *Journal of Geophysical Research: Planets*, 126(5). <https://doi.org/10.1029/2020JE006741>
- Buffo, J. J., Schmidt, B. E., Huber, C., & Walker, C. C. (2020). Entrainment and dynamics of ocean-derived impurities within Europa's ice shell. *Journal of Geophysical Research: Planets*, 125(10), 1–23. <https://doi.org/10.1029/2020JE006394>
- Čadež, O., Kalousová, K., Kworka, J., & Sotin, C. (2021). The density structure of Titan's outer ice shell. *Icarus*, 364, 114466. <https://doi.org/10.1016/j.icarus.2021.114466>
- Carlson, R., Anderson, M., Johnson, R., Smythe, W., Hendrix, A., Barth, C., et al. (1999). Hydrogen peroxide on the surface of Europa. *Science*, 283(5410), 2062–2064. <https://doi.org/10.1126/science.283.5410.2062>
- Carnahan, E., Wolfenbarger, N., Jordan, J., & Hesse, M. (2021). New insights into temperature-dependent ice properties and their effect on ice shell convection for icy ocean worlds. *Earth and Planetary Science Letters*, 563, 116886. <https://doi.org/10.1016/j.epsl.2021.116886>
- Choukroun, M., Grasset, O., Tobie, G., & Sotin, C. (2010). Stability of methane clathrate hydrates under pressure: Influence on outgassing processes of methane on Titan. *Icarus*, 205(2), 581–593. <https://doi.org/10.1016/j.icarus.2009.08.011>
- Choukroun, M., Kieffer, S. W., Lu, X., & Tobie, G. (2013). Clathrate hydrates: Implications for exchange processes in the outer solar system. In *The Science of Solar System Ices* (pp. 409–454). Springer. https://doi.org/10.1007/978-1-4614-3076-6_12
- Choukroun, M., & Sotin, C. (2012). Is Titan's shape caused by its meteorology and carbon cycle? *Geophysical Research Letters*, 39(4). <https://doi.org/10.1029/2011GL050747>
- Durham, W. B., Kirby, S. H., Stern, L. A., & Zhang, W. (2003). The strength and rheology of methane clathrate hydrate. *Journal of Geophysical Research*, 108(B4). <https://doi.org/10.1029/2002JB001872>
- Durham, W. B., Prieto-Ballesteros, O., Goldsby, D. L., & Kargel, J. S. (2010). Rheological and thermal properties of icy materials. *Space Science Reviews*, 153(1–4), 273–298. <https://doi.org/10.1007/s11214-009-9619-1>
- Durham, W. B., Stern, L. A., Kubo, T., & Kirby, S. H. (2005). Flow strength of highly hydrated Mg- and Na-sulfate hydrate salts, pure and in mixtures with water ice, with application to Europa. *Journal of Geophysical Research: Planets*, 110(12), 1–10. <https://doi.org/10.1029/2005JE002475>
- Feistel, R., & Wagner, W. (2006). A new equation of state for H₂O ice Ih. *Journal of Physical and Chemical Reference Data*, 35(2), 1021–1047. <https://doi.org/10.1063/1.2183324>
- Formisano, M., Federico, C., Castillo-Rogez, J., De Sanctis, M. C., & Magni, G. (2020). Thermal convection in the crust of the dwarf planet—I. Ceres. *Monthly Notices of the Royal Astronomical Society*, 494(4), 5704–5712. <https://doi.org/10.1093/mnras/staa1115>

- Fu, R., Ermakov, A., Marchi, S., Castillo-Rogez, J., Raymond, C., Hager, B. H., et al. (2017). The interior structure of Ceres as revealed by surface topography. *Earth and Planetary Science Letters*, 476, 153–164. <https://doi.org/10.1016/j.epsl.2017.07.053>
- Fulle, M., Della Corte, V., Rotundi, A., Rietmeijer, F. J., Green, S. F., Weissman, P., et al. (2016). Comet 67P/Churyumov-Gerasimenko preserved the pebbles that formed planetesimals. *Monthly Notices of the Royal Astronomical Society*, 462, S132–S137. <https://doi.org/10.1093/mnras/stw2299>
- Goldsby, D. L., & Kohlstedt, D. L. (2001). Superplastic deformation of ice: Experimental observations. *Journal of Geophysical Research*, 106(B6), 11017–11030. <https://doi.org/10.1029/2000JB900336>
- Hammond, N. P., Barr, A. C., & Parmentier, E. M. (2016). Recent tectonic activity on Pluto driven by phase changes in the ice shell. *Geophysical Research Letters*, 43(13), 6775–6782. <https://doi.org/10.1002/2016GL069220>
- Hand, K., Chyba, C., Carlson, R., & Cooper, J. (2006). Clathrate hydrates of oxidants in the ice shell of Europa. *Astrobiology*, 6(3), 463–482. <https://doi.org/10.1089/ast.2006.6.463>
- Helgerud, M. B., Waite, W. F., Kirby, S. H., & Nur, A. (2009). Elastic wave speeds and moduli in polycrystalline ice Ih, sI methane hydrate, and sII methane-ethane hydrate. *Journal of Geophysical Research*, 114(B2), B02212. <https://doi.org/10.1029/2008JB006132>
- Hemingway, D., Nimmo, F., Zebker, H., & Iess, L. (2013). A rigid and weathered ice shell on Titan. *Nature*, 500(7464), 550–552. <https://doi.org/10.1038/nature12400>
- Hendrix, A. R., Hurford, T. A., Barge, L. M., Bland, M. T., Bowman, J. S., Brinckerhoff, W., et al. (2019). The NASA roadmap to ocean worlds. *Astrobiology*, 19, 1–27. <https://doi.org/10.1089/ast.2018.1955>
- Hesse, M. A., & Castillo-Rogez, J. C. (2019). Thermal evolution of the impact-induced cryomagma chamber beneath Occator crater on Ceres. *Geophysical Research Letters*, 46(3), 1121–1221. <https://doi.org/10.1029/2018GL080327>
- Howell, S. (2021). The likely thickness of Europa's icy shell. *Planetary Science Journal*, 2(4), 129. <https://doi.org/10.3847/PSJ/abfe10>
- Howell, S., & Pappalardo, R. (2018). Band formation and ocean-surface interaction on Europa and Ganymede. *Geophysical Research Letters*, 45(10), 4701–4709. <https://doi.org/10.1029/2018GL077594>
- Ismail-Zadeh, A., & Tackley, P. (2010). *Computational methods for geodynamics* (1st ed.). Cambridge University Press.
- Ji, S. (2004). A generalized mixture rule for estimating the viscosity of solid-liquid suspensions and mechanical properties of polyphase rocks and composite materials. *Journal of Geophysical Research*, 109(10), 1–18. <https://doi.org/10.1029/2004JB003124>
- Journaux, B., Kalousová, K., Sotin, C., Tobie, G., Vance, S., Saur, J., et al. (2020). Large ocean worlds with high-pressure ices. *Space Science Reviews*, 216. <https://doi.org/10.1007/s11214-019-0633-7>
- Kalousová, K., & Sotin, C. (2020). The insulating effect of methane clathrate crust on Titan's thermal evolution. *Geophysical Research Letters*, 47. <https://doi.org/10.1029/2020GL087481>
- Kamata, S., Nimmo, F., Sekine, Y., Kuramoto, K., Noguchi, N., Kimura, J., & Tani, A. (2019). Pluto's ocean is capped and insulated by gas hydrates. *Nature Geoscience*, 1, 407–410. <https://doi.org/10.1038/s41561-019-0369-8>
- Leitner, M. A., & Lunine, J. I. (2019). Modeling early Titan's ocean composition. *Icarus*, 333, 61–70. <https://doi.org/10.1016/j.icarus.2019.05.008>
- Loveday, J. S., Nelmes, R. J., Guthrie, M., Belmonte, S. A., Allan, D. R., Klug, D. D., et al. (2001). Stable methane hydrate above 2 GPa and the source of Titan's atmospheric methane. *Nature*, 410(6829), 661–663. <https://doi.org/10.1038/35070513>
- Lunine, J. I., & Stevenson, D. J. (1987). Clathrate and ammonia hydrates at high pressure: Application to the origin of methane on Titan. *Icarus*, 70(1), 61–77. [https://doi.org/10.1016/0019-1035\(87\)90075-3](https://doi.org/10.1016/0019-1035(87)90075-3)
- Marounina, N., & Rogers, L. A. (2019). Internal structure and CO₂ reservoirs of habitable water-worlds. *arXiv:1904.10458 [astro-ph]*. Retrieved from <http://arxiv.org/abs/1904.10458>
- McKinnon, W., Simonelli, D., & Schubert, G. (1997). In S. Stern & D. Tholen (Eds.), *Pluto and Charon* (pp. 259–343). University of Arizona Press.
- McKinnon, W., Stern, S., Weaver, H., Nimmo, F., Bierson, C., Grundy, W., et al. (2017). Origin of the Pluto–Charon system: Constraints from the New Horizons flyby. *Icarus*, 287, 2–11. <https://doi.org/10.1016/j.icarus.2016.11.019>
- McKinnon, W. B., Nimmo, F., Wong, T., Schenk, P. M., White, O. L., Roberts, J. H., et al. (2016). Convection in a volatile nitrogen-ice-rich layer drives Pluto's geological vigour. *Nature*, 534(7605), 82–85. <https://doi.org/10.1038/nature18289>
- Miller, K. E., Glein, C. R., & Waite, J. H. (2019). Contributions from accreted organics to Titan's atmosphere: New insights from cometary and chondritic data. *The Astrophysical Journal*, 871(1), 59. <https://doi.org/10.3847/1538-4357/aaf561>
- Mitri, G., Meriggiola, R., Hayes, A., Lefevre, A., Tobie, G., Genova, A., et al. (2014). Shape, topography, gravity anomalies and tidal deformation of Titan. *Icarus*, 236, 169–177. <https://doi.org/10.1016/j.icarus.2014.03.018>
- Moore, P. L. (2014). Deformation of debris-ice mixtures. *Reviews of Geophysics*, 52(3), 435–467. <https://doi.org/10.1002/2014RG000453>
- Mousis, O., Chassefière, E., Holm, N. G., Bouquet, A., Waite, J. H., Geppert, W. D., et al. (2015). Methane clathrates in the solar system. *Astrobiology*, 15(4), 308–326. <https://doi.org/10.1089/ast.2014.1189>
- Mousis, O., Lakhlifi, A., Picaud, S., Pasek, M., & Chassefière, E. (2013). On the abundances of noble and biologically relevant gases in Lake Vostok, Antarctica. *Astrobiology*, 13(4), 380–390. <https://doi.org/10.1089/ast.2012.0907>
- Néri, A., Guyot, F., Reynard, B., & Sotin, C. (2020). A carbonaceous chondrite and cometary origin for icy moons of Jupiter and Saturn. *Earth and Planetary Science Letters*, 530, 115920. <https://doi.org/10.1016/j.epsl.2019.115920>
- Neumann, W., Jaumann, R., Castillo-Rogez, J., Raymond, C. A., & Russell, C. T. (2020). Ceres' partial differentiation: Undifferentiated crust mixing with a water-rich mantle. *Astronomy and Astrophysics*, 633, A117. <https://doi.org/10.1051/0004-6361/201936607>
- Nimmo, F., Hamilton, D. P., McKinnon, W. B., Schenk, P. M., Binzel, R. P., Bierson, C. J., et al. (2016). Reorientation of Sputnik Planitia implies a subsurface ocean on Pluto. *Nature*, 540, 94–96. <https://doi.org/10.1038/nature20148>
- Nimmo, F., Pappalardo, R. T., & Giese, B. (2003). On the origins of band topography, Europa. *Icarus*, 166(1), 21–32. <https://doi.org/10.1016/j.icarus.2003.08.002>
- Peters, B., Zimmermann, N. E., Beckham, G. T., Tester, J. W., & Trout, B. L. (2008). Path sampling calculation of methane diffusivity in natural gas hydrates from a water-vacancy assisted mechanism. *Journal of the American Chemical Society*, 130(51), 17342–17350. <https://doi.org/10.1021/ja802014m>
- Richards, M. A., & Hager, B. H. (1984). Geoid anomalies in a dynamic Earth. *Journal of Geophysical Research*, 89(B7), 5987–6002. <https://doi.org/10.1029/JB089iB07p05987>
- Robuchon, G., & Nimmo, F. (2011). Thermal evolution of Pluto and implications for surface tectonics and a subsurface ocean. *Icarus*, 216(2), 426–439. <https://doi.org/10.1016/j.icarus.2011.08.015>
- Sloan, E. D., & Koh, C. (2007). *Clathrate hydrates of natural gases* (3rd ed.). CRC Press.
- Soderlund, K. M., Kalousová, K., Buffo, J. J., Glein, C. R., Goodman, J. C., Mitri, G., et al. (2020). Ice-Ocean exchange processes in the Jovian and Saturnian satellites. *Space Science Reviews*, 216(5), 80. <https://doi.org/10.1007/s11214-020-00706-6>

- Takeda, Y.-T. (1998). Flow in rocks modelled as multiphase continua: Application to polymineralic rocks. *Journal of Structural Geology*, 20(11), 1569–1578. [https://doi.org/10.1016/S0191-8141\(98\)00043-1](https://doi.org/10.1016/S0191-8141(98)00043-1)
- Tobie, G., Choblet, G., & Sotin, C. (2003). Tidally heated convection: Constraints on Europa's ice shell thickness. *Journal of Geophysical Research*, 108(E11), 5124. <https://doi.org/10.1029/2003JE002099>
- Tobie, G., Lunine, J. I., & Sotin, C. (2006). Episodic outgassing as the origin of atmospheric methane on Titan. *Nature*, 440(7080), 61–64. <https://doi.org/10.1038/nature04497>
- Trumbo, S. K., Brown, M. E., & Hand, K. P. (2019). Sodium chloride on the surface of Europa. *Science Advances*, 5(6), eaaw7123. <https://doi.org/10.1126/sciadv.aaw7123>
- Vance, S. D., Panning, M. P., Stähler, S., Cammarano, F., Bills, B. G., Tobie, G., et al. (2018). Geophysical investigations of habitability in ice-covered ocean worlds: Geophysical habitability. *Journal of Geophysical Research: Planets*, 123(1), 180–205. <https://doi.org/10.1002/2017JE005341>
- Vilella, K., Choblet, G., Tsao, W., & Deschamps, F. (2020). Tidally heated convection and the occurrence of melting in icy satellites: Application to Europa. *Journal of Geophysical Research: Planets*, 125(3). <https://doi.org/10.1029/2019JE006248>
- Wells, A. J., Hitchen, J. R., & Parkinson, J. R. (2019). Mushy-layer growth and convection, with application to sea ice. *Philosophical Transactions of the Royal Society A: Mathematical, Physical & Engineering Sciences*, 377(2146). <https://doi.org/10.1098/rsta.2018.0165>
- Wolfenbarger, N. S., Carnahan, E., Jordan, J. S., & Hesse, M. A. (2021). A comprehensive dataset for the thermal conductivity of ice Ih for application to planetary ice shells. *Data in Brief*, 36, 107079. <https://doi.org/10.1016/j.dib.2021.107079>

References From the Supporting Information

- Ashkenazy, Y. (2019). The surface temperature of Europa. *Heliyon*, 5(6), e01908. <https://doi.org/10.1016/j.heliyon.2019.e01908>
- Brumby, P. E., Yuhara, D., Wu, D. T., Sum, A. K., & Yasuoka, K. (2016). Cage occupancy of methane hydrates from Gibbs ensemble Monte Carlo simulations. *Fluid Phase Equilibria*, 413, 242–248. <https://doi.org/10.1016/j.fluid.2015.10.005>
- Earle, A., Binzel, R., Young, L., Stern, S., Ennico, K., Grundy, W., et al. (2017). Long-term surface temperature modeling of Pluto. *Icarus*, 287, 37–46. <https://doi.org/10.1016/j.icarus.2016.09.036>
- Hobbs, P. (1974). *Ice physics*. Clarendon Press.
- Howell, S., & Pappalardo, R. (2020). NASA's Europa Clipper—A mission to a potentially habitable ocean world. *Nature Communications*, 11(1), 9–12. <https://doi.org/10.1038/s41467-020-15160-9>
- Jennings, D., Cottini, V., Nixon, C., Achterberg, R., Flasar, F., Kunde, V., et al. (2016). Surface temperatures on Titan during northern winter and spring. *The Astrophysical Journal*, 816(1), L17. <https://doi.org/10.3847/2041-8205/816/1/L17>
- Jia, J., Liang, Y., Tsuji, T., Murata, S., & Matsuoka, T. (2017). Elasticity and stability of clathrate hydrate: Role of guest molecule motions. *Scientific Reports*, 7. <https://doi.org/10.1038/s41598-017-01369-0>
- Journaux, B., Brown, J. M., Pakhomova, A., Collings, I. E., Petitgirard, S., Espinoza, P., et al. (2020). Holistic approach for studying planetary hydrospheres: Gibbs representation of ices thermodynamics, elasticity, and the water phase diagram to 2,300 MPa. *Journal of Geophysical Research: Planets*, 125(1), e2019JE006176. <https://doi.org/10.1029/2019JE006176>
- LeVeque, R. (2002). *Finite volume methods for hyperbolic problems*. Cambridge University Press.
- Wagner, W., Riethmann, T., Feistel, R., & Harvey, A. H. (2011). New equations for the sublimation pressure and melting pressure of H₂O ice Ih. *Journal of Physical and Chemical Reference Data*, 40(4), 043103. <https://doi.org/10.1063/1.3657937>